Statistics of Multiple Particle Breakage

Priscilla J. Hill and Ka M. Ng
Dept. of Chemical Engineering, University of Massachusetts, Amherst, MA 01003

A method for generating theoretical breakage distribution functions for multiple particle breakage is presented. It starts with the joint probability function that accounts for all the child particles; it is then reduced to the marginal probability function commonly used in the breakage equation. This method is flexible enough to allow the user to choose the number of child particles and the functional form to be used. The method is demonstrated with both product and summation functions with a power-law form. To facilitate the use of these theoretical functions for statistical analyses, a companion discretized breakage equation is developed. The new equation guarantees the conservation of mass and correct prediction of the total number of particles despite discretization. It is easy to use because it is a set of ordinary differential equations and applicable to both equal-size and geometric-size intervals. Simulation results show that different breakage distribution functions coupled with different breakage rates can produce almost indistinguishable particle-size distributions, signifying the need for further work in this area.

Introduction

Breakage is a common occurrence in science as well as in engineering. Depending on the situation, the same phenomenon is referred to as crushing, grinding, fracture, partition, division, disintegration, shattering, scission, fragmentation, degradation, and abrasion. In the chemical processing industry, breakage can strongly influence the operation and economics of a manufacturing process. For example, fragmentation of catalyst particles in a gas–solid fluid bed is deleterious to reactor performance. Dust formation due to attrition of solid particles in a rotary drum dryer may lead to an explosion. Breakage of solid particles in a pump or a control valve may lead to blockage. However, not all breakage is undesirable. In mineral processing, crushing is necessary to obtain particles of sizes suitable for further processing. Grinding of the crystalline pharmaceutical products after a crystallization step is often performed before tabletting.

To quantify breakage for process design and optimization, two pieces of information are needed—the rate at which breakage occurs and the number and sizes of the child particles resulting from the breakage of a parent particle. Both are accounted for in the commonly used number-based breakage equation for a batch process.

$$\frac{dn(v)}{dt} = \int_v^\infty b'(v,w)S(w)n(w)\,dw - S(v)n(v). \qquad (1)$$

Correspondence concerning this article should be addressed to K. M. Ng.

Here, $n(v)$ is the number density function, t is the time, v and w are particle volumes, $S(v)$ is the specific rate of breakage, and $b'(v, w)$ is the number-based breakage distribution function. Equation 1 is valid for breakage with two or more child particles, but the prime is used to signify our focus on breakage distribution functions with three or more child particles in this article. For binary breakage, the prime is omitted and $b(v, w)$ is a symmetric function, reflecting the fact that when a child particle is of size v, the other child particle must be of size $w - v$. Symmetry does not exist for $b'(v, w)$ in general.

The specific rate of breakage and/or the breakage distribution function have been determined empirically for a number of process units and materials; a partial listing is given in Table 1. The typical approach for determining the breakage distribution function is as follows. First, functional forms with a number of adjustable parameters are assumed. Then, data on the particle-size distribution (PSD) are obtained at various times as breakage progresses. The adjustable parameters that fit the data the best are back-calculated using various schemes (Klimpel and Austin, 1970, 1984; Austin and Luckie, 1971/72a,b). One such mass-based empirical breakage distribution function (Austin et al., 1976) is

$$B_M(v,w) = \phi\left(\frac{v}{w}\right)^{\gamma/3} + (1-\phi)\left(\frac{v}{w}\right)^{\beta/3} \qquad (2)$$

Table 1. Breakage Parameters for Process Equipment

Equipment Unit	Experimental Parameters	Materials	Reference
Crushers			
Ball mill	mill rotation speed, ball size	quartz, limestone, silicon carbide, cement clinker	
Vibration ball mill	vibration amplitude and frequency	silicon carbide	Austin et al. (1976)
Rod mill	rod size	cement clinker	
Stirred Tank	magma density, power input,	copper sulfate crystals, nickel ammonium crystals	Nienow and Conti (1978)
	fluid viscosity, fluid density, magma density, aggregate size	kaolin–anionic polymer flocs	Glasgow and Luecke (1980)
	stirring rate, crystal shape factor, magma density	potassium sulfate crystals	Mazzarotta (1992)
	power input, magma density, crystal shape factor	potassium sulfate crystals, potash alum crystals	Synowiec et al. (1993)
Pipeline	shear rate	coal	Karabelas (1976)
Fluid catalytic cracker	residence time	catalyst	Wei et al. (1977)
Ribbon mixer	rotation speed, moisture content	sea sand	Masiuk (1987)
Pumps			
Centrifugal	rotation speed	lignite	Shook et al. (1978)
Axial flow	rotation speed, impeller diameter	sodium chloride	Offermann and Ulrich (1982)
Gear, screw, peristaltic, centrifugal	shear rate	soya protein precipitates	Hoare et al. (1982)
Ultrasonic disrupter	ultrasonic power input	silica agglomerates, titania agglomerates	Kusters et al. (1993)

Here, $B_M(v, w)$ is the cumulative mass-breakage function. The corresponding number-based breakage distribution function (Hill and Ng, 1995) is

$$b'(v,w) = \frac{\phi\gamma}{3w}\left(\frac{v}{w}\right)^{(\gamma/3)-2} + \frac{(1-\phi)\beta'}{3w}\left(\frac{v}{w}\right)^{(\beta'/3)-2}. \quad (3)$$

The adjustable parameters γ, β', and ϕ depend on the material being ground and on the type of equipment. For materials such as silicon carbide, quartz, cement clinker, and limestone, γ ranges from 0.59 to 1.17, β' from 3.2 to 4.7, and ϕ from 0.2 to 0.36.

In addition to the empirical breakage distribution functions, a number of expressions amenable to mathematical analysis have been suggested for studying the statistics of breakage in a general way. The simplest is the uniform function that implies that it is equally likely to form a child particle of any size less than that of the parent particle. Other examples include the parabolic function for binary breakage (Hill and Ng, 1995) and the following functions for multiple-particle breakage (Ziff, 1991):

$$b(v,w) = -\frac{\lambda^2}{w}\left(\frac{v}{w}\right)^{\lambda-2}\ln\left(\frac{v}{w}\right) \quad (4)$$

and

$$b'(v,w) = \frac{\phi\lambda}{w}\left(\frac{v}{w}\right)^{\lambda-2} + (1-\phi)\frac{\eta}{w}\left(\frac{v}{w}\right)^{\eta-2}. \quad (5)$$

Equation 5 is sufficiently general in that it represents a number of the expressions reported in the literature. Interestingly, we note that Eq. 5 is identical to the empirical function, Eq. 3, with $\lambda = \gamma/3$ and $\eta = \beta'/3$.

Rather than just assuming a breakage distribution function to represent the overall outcome of a number of simultaneous fragmentations, the statistics for multiple-particle breakage can be analyzed in more detail. For example, Davis (1989) developed two breakage models, a remaining-piece breakage model and a cascade breakage model. The former assumes cessation of breakage for some child particles while the latter does not. The distribution of the lengths of the segments resulting from partitioning a line is available in Feller (1966). More general fragmentation statistics were considered by Grady (1990).

The objective of this article is to explain a procedure for deriving breakage distribution functions and to investigate the statistics of multiple particle breakage. Basically, the breakage distribution function $b'(v, w)$ is a marginal probability;

the intrinsic probability for breakage is masked. Instead, we begin with the joint probability which, as in the statistical analyses mentioned earlier, considers all the child particles. To fix ideas, we first show how to develop breakage distribution functions for ternary breakage. Then the method is extended to include any number of child particles. This is followed by a comparison of these theoretical expressions with the empirical functions. Finally, we examine the size distribution of the child particles resulting from these theoretical expressions after solving Eq. 1 using a new discretization procedure.

Ternary Breakage

Let three child particles have volumes v_1, v_2, and v_3, while the parent particle is of volume w. To conserve volume, we have the following constraint:

$$v_1 + v_2 + v_3 = w. \tag{6}$$

The breakage function $b(v_1, v_2, w)$ is used to represent the probability of forming particles of volumes v_1 and v_2, given that a particle of volume w breaks. Since v_3 can be determined from the sizes of the parent particle and the other two child particles, it does not explicitly appear in this function.

When the parent particle breaks, the first child particle, v_1, may range in volume from zero to w. Once v_1 is fixed, the second child particle, v_2, may range in volume from zero to $w - v_1$. Thus, the relation between the marginal probability $b'(v, w)$ and the joint probability function $b(v_1, v_2, w)$ is

$$b'(v_1,w) = \int_0^{w-v_1} b(v_1,v_2,w)\,dv_2. \tag{7}$$

And a more complete form of Eq. 1 for ternary breakage is

$$\frac{dn(v_1)}{dt} = \int_{v_1}^{\infty}\int_0^{w-v_1} b(v_1,v_2,w)S(w)n(w)\,dv_2\,dw - S(v_1)n(v_1). \tag{8}$$

There are several constraints on the functional form of $b(v_1,v_2,w)$. To predict three child particles, we have

$$\int_0^w \int_0^{w-v_1} b(v_1,v_2,w)\,dv_2\,dv_1 = 3. \tag{9}$$

The mass breakage function $b'_M(v_1, w)$ is related to the number breakage function $b'(v_1,w)$ by

$$b'_M(v_1,w) = \frac{v_1}{w} b'(v_1,w). \tag{10}$$

Therefore, for conservation of mass, we also have

$$\int_0^w \int_0^{w-v_1} \frac{v_1}{w} b(v_1,v_2,w)\,dv_2\,dv_1 = 1. \tag{11}$$

In addition, since v_1, v_2, and v_3 are exchangeable variables (Feller, 1966), we have

$$\begin{aligned} b(v_1,v_2,w) &= b(v_1,v_3,w) = b(v_2,v_1,w) \\ &= b(v_2,v_3,w) = b(v_3,v_1,w) \\ &= b(v_3,v_2,w). \end{aligned} \tag{12}$$

That is, the distribution function should not depend on which particle volume is first, second, and third.

Functional forms for $b(v_1, v_2, w)$

To meet these constraints, functions can be of the following general form:

$$b(v_1,v_2,w) = \frac{A[f(v_1)\otimes f(v_2)\otimes f(v_3)]}{g(w)}, \tag{13}$$

where $\otimes$ indicates an operation such as multiplication or addition. For the breakage function to observe exchangeability with respect to the child particle volumes, the same function f is used for each child particle. It can be of a power law form, a trigonometric, logarithmic, or exponential function. The righthand sides of Eqs. 9 and 11 are not functions of the parent particle size. The constant A and the normalization function $g(w)$ are determined by substituting Eq. 13 into either equation to ensure the correct number of child particles and mass conservation.

Other alternatives exist. For example, instead of being limited to one variable, the function f can be a symmetric function of two variables to yield

$$b(v_1,v_2,w) = \frac{A[f(v_1,v_2)f(v_2,v_3)f(v_3,v_1)]}{g(w)} \tag{14}$$

or

$$b(v_1,v_2,w) = \frac{A[f(v_1,v_2)+f(v_2,v_3)+f(v_3,v_1)]}{g(w)}. \tag{15}$$

Product function with a power-law form

To illustrate the procedure for deriving breakage distribution functions, let us consider the specific case where the operation in Eq. 13 is multiplication. Thus, we have

$$b(v_1,v_2,w) = \frac{Af(v_1)f(v_2)f(v_3)}{g(w)}. \tag{16}$$

Further, assuming a power-law form for the function f, we get

$$b(v_1,v_2,w) = \frac{A_m v_1^m v_2^m (w - v_1 - v_2)^m}{w^{3m+2}}. \tag{17}$$

Since the constant A in Eq. 16 varies with the exponent m, the value of A that corresponds with a given value of m is

denoted as A_m. To determine A_m, the expression for $b(v_1, v_2, w)$ is substituted into either Eq. 9 or Eq. 11. If m is a nonnegative integer, then A_m is given by

$$A_m = \frac{3}{\sum_{k=0}^{m} \binom{m}{k} (-1)^k \frac{1}{m+k+1} \sum_{j=0}^{2m+1} \binom{2m+1}{j} (-1)^j \frac{1}{m+j+1}} \tag{18}$$

or

$$A_m = \frac{1}{\sum_{k=0}^{m} \binom{m}{k} (-1)^k \frac{1}{m+k+1} \sum_{j=0}^{2m+1} \binom{2m+1}{j} (-1)^j \frac{1}{m+j+2}} \tag{19}$$

for the number prediction and mass conservation equations, respectively. These expressions may be simplified using the following relation (Jolley, 1961):

$$\sum_{k=0}^{n} \binom{n}{k} (-1)^k \frac{1}{k+h} = \frac{n!(h-1)!}{(n+h)!}. \tag{20}$$

After simplification, we get the same result of

$$A_m = \frac{3(3m+2)!}{(m!)^3}. \tag{21}$$

As expected, the two expressions are equivalent. In general, we can show by substituting Eq. 17 into Eq. 7 that

$$b'(v,w) = \frac{3v^m (w-v)^{2m+1} (3m+2)!}{w^{3m+2} (2m+1)! m!}. \tag{22}$$

Some examples of A_m, m, and $b'(v, w)$ are given in Table 2.

Table 2. Product Form of $b'(v, w)$ and A for $m = -1/2$, 0, 1, and 2

m	A	$b'(v,w)$
$-1/2$	$\frac{3}{2[\sin^{-1}(1) - \sin^{-1}(-1)]}$	$\frac{3}{2} v^{-1/2} w^{-1/2}$
0	6	$\frac{6(w-v)}{w^2}$
1	360	$\frac{60v(w-v)^3}{w^5}$
2	15,120	$\frac{504v^2(w-v)^5}{w^8}$

Summation function with a power-law form

Another way to meet the constraints is to use a function of the form

$$b(v_1, v_2, w) = \frac{A[f(v_1) + f(v_2) + f(v_3)]}{g(w)}. \tag{23}$$

Again, any function can be chosen for f, but if a power-law form is assumed, we get

$$b(v_1, v_2, w) = \frac{A[v_1^m + v_2^m + (w - v_1 - v_2)^m]}{w^{m+2}}. \tag{24}$$

If m is a nonnegative integer, then A_m is given by

$$A_m = \frac{3}{\frac{1}{m+1} - \frac{1}{m+2} + \left[\frac{1}{m+1} + \frac{1}{m+1}\right] \frac{1}{m+2}} \tag{25}$$

or

$$A_m = \frac{1}{\frac{1}{m+2} - \frac{1}{m+3} + \left[\frac{2}{m+1}\right] \sum_{j=0}^{m+1} \binom{m+1}{j} (-1)^j \frac{1}{j+2}} \tag{26}$$

using Eqs. 9 and 11, respectively. Equations 25 and 26 can be simplified using Eq. 20 to yield

$$A_m = (m+1)(m+2). \tag{27}$$

In general, we can show by substituting Eq. 24 into Eq. 7 that

$$b'(v,w) = \frac{(m+1)(m+2)\left[v^m (w-v) + \frac{2}{m+1}(w-v)^{m+1}\right]}{w^{m+2}}. \tag{28}$$

Some examples of A_m, m, and $b'(v, w)$ are given in Table 3.

Table 3. Summation Form of $b'(v,w)$ and A for $m = 0$, 1, 2, and 3

m	A	$b'(v,w)$
0	2	$\frac{6(w-v)}{w^2}$
1	6	$\frac{6(w-v)}{w^2}$
2	12	$\frac{8w^3 - 24vw^2 + 36v^2w - 20v^3}{w^4}$
3	20	$\frac{10(w^4 - 4vw^3 + 6v^2w^2 - 2v^3w - v^4)}{w^5}$

Multiple Breakage

The approach is now generalized to the case where p child particles are formed from the breakage of one parent particle. The general form of the constraint for volume conservation is

$$\sum_{i=1}^{p} v_i = w. \tag{29}$$

The breakage distribution function, $b(v_1, v_2, \ldots, v_{p-1}, w)$, is the expected size distribution of p child particles given that a particle of size w breaks. Since v_p can be determined from the parent particle size and the sizes of the other child particles, it is not explicitly included in this breakage function.

When particle breakage occurs, the first particle can range in size from 0 to w, the second can range in size from 0 to $w - v_1$, and so on. This process is repeated with the requirement that the volume of the next child particle cannot exceed the remaining volume. Thus, the relation of the marginal probability $b'(v, w)$ to the joint probability function $b(v_1, v_2, \ldots, v_{p-1}, w)$ is

$$b'(v_1,w) = \int_0^{w-v_1}\int_0^{w-v_1-v_2}\cdots\int_0^{w-\sum_{i=1}^{p-2}v_i} \times b(v_1,v_2,\ldots,v_{p-1},w)\,dv_{p-1}\ldots dv_3 dv_2. \tag{30}$$

A more complete form of Eq. 1 is

$$\frac{dn(v_1)}{dt} = -S(v_1)n(v_1) + \int_{v_1}^{\infty}\int_0^{w-v_1}\int_0^{w-v_1-v_2}\cdots\int_0^{w-\sum_{i=1}^{p-2}v_i} \times b(v_1,v_2,\ldots,v_{p-1},w)S(w)n(w)\,dv_{p-1}\ldots dv_3 dv_2 dw. \tag{31}$$

Again, there are several requirements that $b(v_1, v_2, \ldots, v_{p-1}, w)$ must meet. In order to predict p child particles, we have

$$\int_0^{w}\int_0^{w-v_1}\int_0^{w-v_1-v_2}\cdots\int_0^{w-\sum_{i=1}^{p-2}v_i} \times b(v_1,v_2,\ldots,v_{p-1},w)\,dv_{p-1}\ldots dv_3 dv_2 dv_1 = p. \tag{32}$$

For conservation of mass, we have

$$\int_0^{w}\int_0^{w-v_1}\int_0^{w-v_1-v_2}\cdots\int_0^{w-\sum_{i=1}^{p-2}v_i}\frac{v_1}{w} \times b(v_1,v_2,\ldots,v_{p-1},w)\,dv_{p-1}\ldots dv_3 dv_2 dv_1 = 1. \tag{33}$$

In addition, we must have exchangeability so that the breakage function does not change if the order of the particles is changed. For breakage with p child particles, an equivalent expression of Eq. 12 consists of $(p! - 1)$ equations.

Product function with a power-law form

A product function is of the following general form:

$$b(v_1,v_2,\ldots,v_{p-1},w) = \frac{Af(v_1)f(v_2)f(v_3)\ldots f(v_p)}{g(w)}. \tag{34}$$

A power-law form of this is

$$b(v_1,v_2,\ldots,v_{p-1},w) = \frac{A_{m,p}v_1^m v_2^m \ldots v_{p-1}^m\left(w - \sum_{i=1}^{p-1} v_i\right)^m}{w^{pm+p-1}}. \tag{35}$$

For nonnegative integer values of m, substitution of Eq. 35 into Eq. 32 yields

$$A_{m,p} = \frac{p}{\prod_{i=1}^{p-1}\sum_{k=0}^{m+(m+1)(i-1)}\binom{m+(m+1)(i-1)}{k}(-1)^k\frac{1}{m+k+1}}. \tag{36}$$

This can be simplified by using Eq. 20 to obtain

$$A_{m,p} = \frac{p[m+(m+1)(p-1)]!}{(m!)^p}. \tag{37}$$

In general, $b'(v, w)$ is

$$b'(v,w) = \frac{pv^m(w-v)^{m+(m+1)(p-2)}}{w^{pm+p-1}\sum_{k=0}^{m+(m+1)(p-2)}\binom{m+(m+1)(p-2)}{k}(-1)^k\frac{1}{m+k+1}}. \tag{38}$$

Again, simplification using Eq. 20 yields

$$b'(v,w) = \frac{pv^m(w-v)^{m+(m+1)(p-2)}[m+(m+1)(p-1)]!}{w^{pm+p-1}m![m+(m+1)(p-2)]!}. \tag{39}$$

For $m = 0$, we have

$$b'(v,w) = \frac{p(w-v)^{(p-2)}(p-1)}{w^{p-1}}. \tag{40}$$

This limiting case represented by Eq. 40 can be found in Feller (1966). For ternary breakage where $p = 3$, Eqs. 37 and 39 simplify to Eqs. 21 and 22, respectively.

Summation function with a power-law form

A general form of the summation function for p particles is

$$b(v_1, v_2, \ldots, v_{p-1}, w) = \frac{A_p\left[\sum_{i=1}^{p-1} f(v_i) + f\left(w - \sum_{i=1}^{p-1} v_i\right)\right]}{g(w)}. \tag{41}$$

For the power-law form of the summation function, the breakage distribution function is

$$b(v_1, v_2, \ldots, v_{p-1}, w) = \frac{A_{m,p}\left[\sum_{i=1}^{p-1} v_i^m + \left(w - \sum_{i=1}^{p-1} v_i\right)^m\right]}{w^{m+p+1}}. \tag{42}$$

For $p = 2$, we have

$$\frac{2}{A_{m,2}} = \frac{2}{m+1}, \tag{43}$$

and for $p > 2$ we have the following recursive relationship:

$$\frac{p}{A_{m,p}} = \frac{(p-2)!m!}{(m+p-1)!}\prod_{i=0}^{p-3}\frac{1}{i+1} + \left(\frac{p-1}{A_{m,p-1}}\right)\frac{1}{m+p-1}. \tag{44}$$

Substituting Eqs. 43 and 44 into either Eq. 32 or 33, we can determine $A_{m,p}$ for $p \geq 2$. For $p = 2$, we get

$$b'(v,w) = \frac{m+1}{w^{m+1}}[v^m + (w-v)^m], \tag{45}$$

and for $p > 2$, we have

$$b'(v,w) = \frac{A_{m,p}}{w^{m+p-1}} \times \left[v^m(w-v)^{p-2}\prod_{i=0}^{p-3}\frac{1}{i+1} + (w-v)^{m+p-2}\left(\frac{p-1}{A_{m,p-1}}\right)\right]. \tag{46}$$

Results

Before proceeding further, let us examine the preceding functional forms of $b'(v, w)$ graphically. In the first set of comparisons, we assume spherical particles with an original particle volume of 5×10^8 μm^3 or a diameter of 985 μm. For $m = 0$, it can be shown using Eqs. 40 and 46 that the product

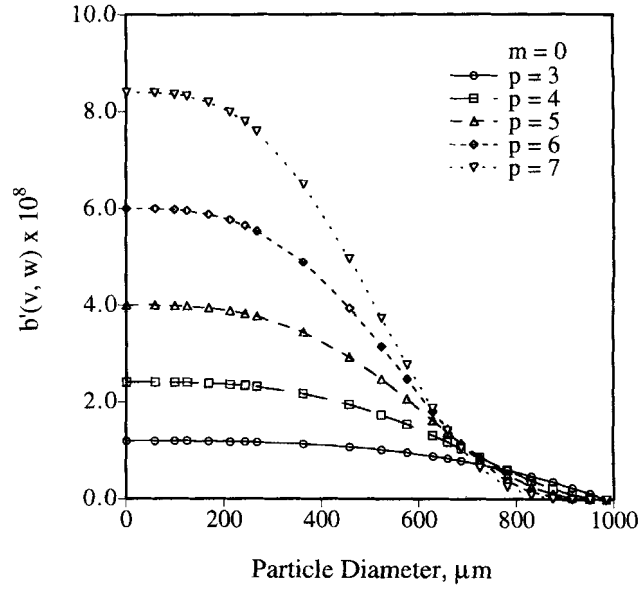

Figure 1. Breakage distribution function for a product or summation function with a power-law exponent of $m = 0$.

and summation breakage functions are the same. Both represent the uniform distribution function where it is equally likely to form a child particle of any size less than that of the parent particle. This uniform breakage distribution function is plotted against particle diameter for various values of the number of child particles in Figure 1. There are two obvious trends. For a fixed value of p, there are more small child particles than large ones. And, as the number of child particles increases, more small particles are formed. Also note that the uniform distribution function predicts a large number of child particles of zero volume, which is usually not a realistic proposition.

Figure 2 shows $b'(v,w)$ for power law factors of $-1/2$, 0, $1/2$, 1 and 2 for the product form of ternary breakage (Table

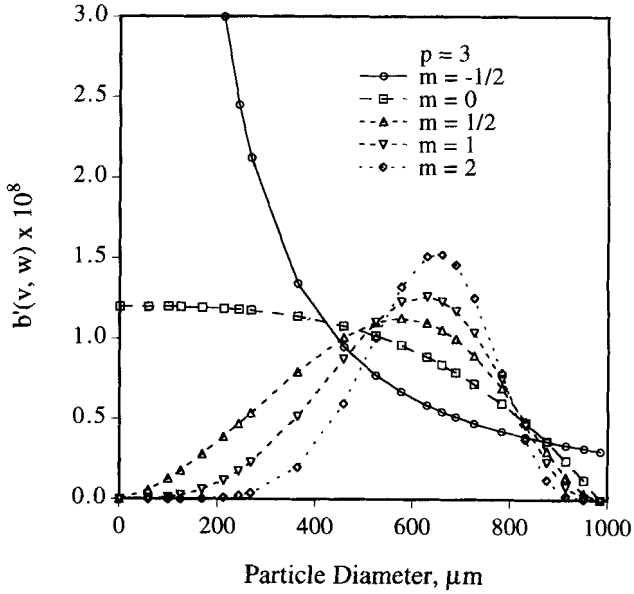

Figure 2. Ternary product breakage distribution function with various power-law exponents.

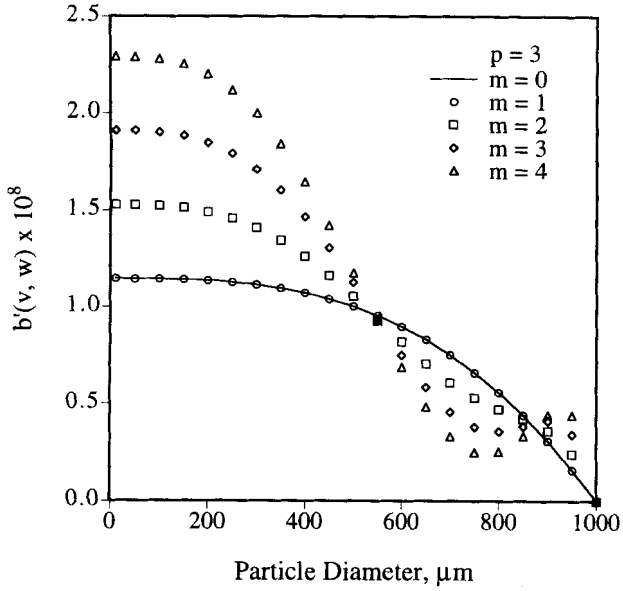

Figure 3. Ternary summation breakage distribution function with various power-law exponents.

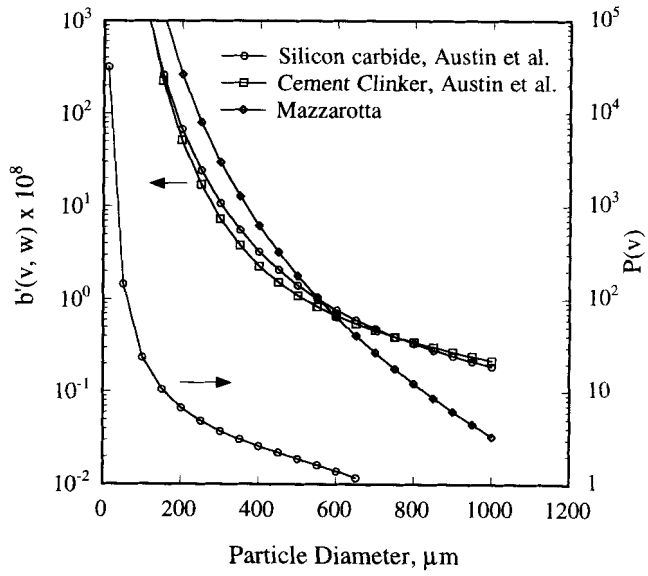

Figure 4. Empirical breakage distribution functions for various substances from Mazzarotta (1992) and Austin et al. (1976).

2). Again, uniform ternary breakage is represented when m is zero. For m larger than zero, there exists a peak that increases in amplitude and shifts to a higher particle diameter as m is increased. Thus, the mean child particle size increases with m. For m equal to $-1/2$, the distribution function is a monotonic decreasing function with particle diameter. It also predicts an infinite number of child particles of zero volume.

Figure 3 shows $b'(v, w)$ for power law factors of 0, 1, 2, 3 and 4 for the summation form of ternary breakage (Table 3). As m is increased from zero, the function goes through an inflection point and then forms a depression around the particle diameter of 750 μm. That is, there are more small and large child particles, but fewer medium-sized child particles.

Comparison with Empirical Distribution Functions

It is interesting to compare some of the empirical distribution functions with the theoretical functions developed earlier. Figure 4 shows three empirical functions due to Austin et al. (1976) and Mazzarotta (1992); the curves were calculated using the original cumulative mass-breakage functions such as Eq. 2. Also shown for the silicon carbide data in Figure 4 is $P(v)$, which is the number of child particles falling between v and the maximum volume. It is determined by integrating the number-based breakage distribution function between the same limits. As can be seen, the number of child particles increases sharply as the particle size decreases below 100 μm. If the empirical correlations are reliable for those small sizes, the number of child particles formed per breakage can run in the thousands. Actually, the first term on the right-hand side of Eq. 3 goes to infinity as v tends to zero.

A comparison of the distribution functions in Figure 4 with those in Figures 1 to 3 shows that the experimental functions cannot be reproduced with the product function or the summation function with a positive power-law exponent. The only curve that has the appropriate shape is the case where $m = -1/2$ for the product function (Figure 2). The breakage functions obtained from the experimental correlations also have the particle volume raised to a negative exponent. Considerable effort was spent, without success, to match the empirical functions using functional forms other than the power law form for f in Eq. 13. We had to conclude that the empirical distribution functions are not compatible with joint probability functions that observe the exchangeability requirement.

This dilemma was solved as follows. It is not physically realistic to expect that the same number of child particles are formed every time a parent particle is broken. Instead, we believe there is a distribution of the number of child particles formed when a particle is broken. That is, the observed experimental breakage function or the composite function is a linear combination of several theoretical breakage functions for various numbers of child particles.

$$b'^{\text{comp}} = \sum_p w_p b'(p). \tag{47}$$

Here, w_p are weighting factors.

To illustrate the matching procedure, let us reexamine the product function with a power-law form. Figures 5a and 5b show the results for exponent values of 0 and 1, respectively, for several values of p. In each case, no one single theoretical curve matches the empirical data. However, each theoretical curve with an increasing p intersects the empirical curve at a progressively smaller particle size. Indeed, as shown in Figure 6, an excellent match is possible with a composite curve using the product form for $m = 0$ (Eq. 48) or $m = 1$ (Eq. 49):

$$\begin{aligned} b'^{\text{comp}} = {} & 0.02b'(5{,}000) + 0.02b'(1{,}000) + 0.026b'(200) \\ & + 0.017b'(100) + 0.05b'(50) + 0.058b'(10) \\ & + 0.12b'(6) + 0.45b'(3) \end{aligned} \tag{48}$$

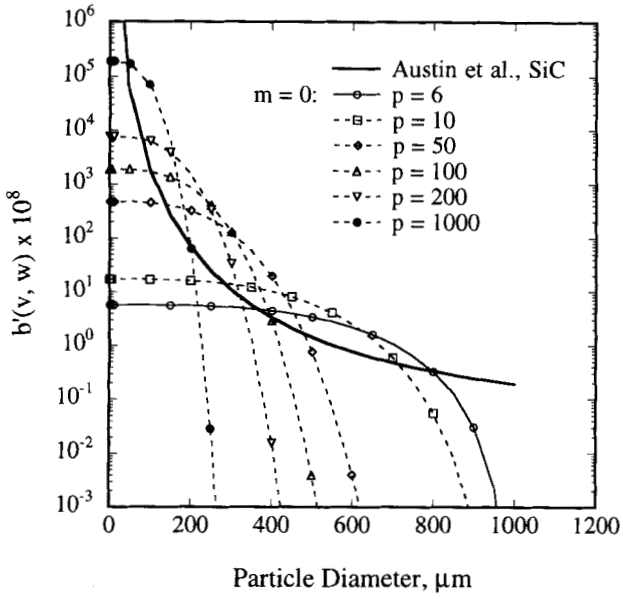

(a)

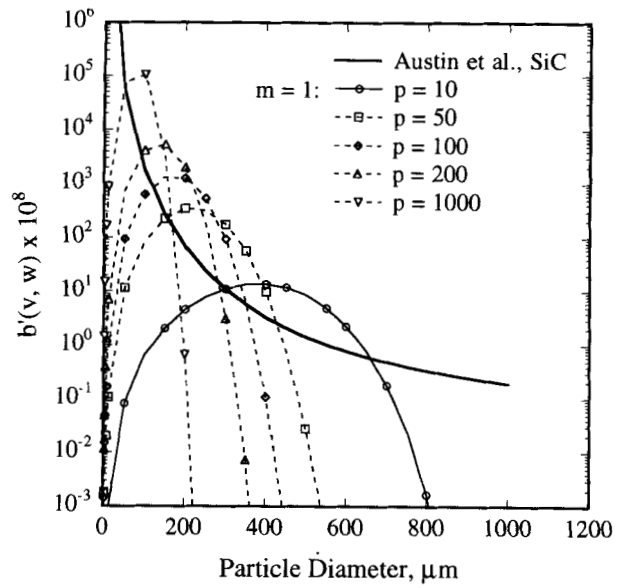

(b)

Figure 5. Empirical breakage functions vs. product function for various values of p: (a) at $m=0$; (b) at $m=1$.

$$b'^{\text{comp}} = 0.02b'(5{,}000) + 0.026b'(1{,}000) + 0.015b'(200) + 0.013b'(100) + 0.058b'(50) + 0.12b'(10) + 0.45b'(3). \quad (49)$$

In both cases, the largest weighting factor is for the case where $p = 3$ and the smaller weighting factors are for the larger values of p. This indicates that most of the particles break into a few child particles. No attempts were made to optimize the matching. The composite curves do not predict the empirical curve when the particles are less than 50 μm. However, terms for $p > 5{,}000$ with small weighting factors may be added to capture the behavior of the curve when the particles are smaller than 50 μm. Neither composite curve predicts an infinite number of child particles of zero volume. For $m = 0$, a finite number of child particles of zero volume exist; for $m = 1$, none exist. Also, adding a term for binary breakage would better predict the behavior near the parent particle size.

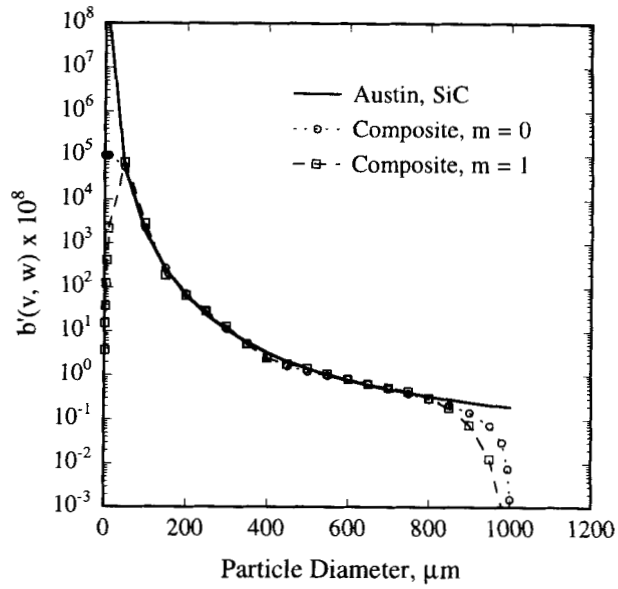

Figure 6. Composite product breakage functions vs. an empirical breakage function.

New Discretized Breakage Equation

We examine next the particle-size distribution resulting from the theoretical functions. In a previous article (Hill and Ng, 1995), we presented a new discretization procedure for the breakage equation, focusing on binary breakage and the empirical breakage models. A general development for multiple particle breakage is now developed below. As before, Eq. 1 is replaced by the following discretized equation:

$$\frac{d}{dt}N_i = \sum_{j=i+1}^{\infty} \beta_j b_{ij} S_j N_j - \delta_i S_i N_i. \quad (50)$$

Here, N_i is the number of particles in size interval i, and β_j and δ_i are the birth and death term factors, respectively. These factors are determined as follows. Setting the time derivative of the first moment of Eq. 50 to zero, we get

$$\delta_i = \frac{\beta_i}{\bar{v}_i} \sum_{j=1}^{i-1} \bar{v}_j b_{ji}. \quad (51)$$

Here $\bar{v}_i$ is any representative size, such as the arithmetic mean, for interval i. This result is applicable for any p and was derived in Hill and Ng as Eq. 32. The time derivative of the zeroth moment for Eq. 1 is

$$\frac{d}{dt}m_0 = (p-1)\int_0^{\infty} S(v)n(v)dv, \quad (52)$$

which holds for all functional forms of $b(v, w)$. Substituting $S(v) = S_c v^{\alpha}$ for $v \geq v_1$ and $S(v) = 0$ for $v < v_1$ into Eq. 52, we get

$$\frac{d}{dt} m_0 = (p-1) S_c (m_\alpha - \overline{v_1^{\alpha}} N_1). \tag{53}$$

The derivations for the time derivative of the zeroth moment are more involved, but parallel Eqs. 41 to 44 and 69 to 71 in Hill and Ng (1995). Following the same steps for Eq. 50, we get

$$\frac{d}{dt} m_0 = \sum_{i=1}^{\infty} \beta_i \left(p - \frac{1}{\bar{v}_i} \sum_{j=1}^{i-1} \bar{v}_j b_{ji} \right) S_i N_i. \tag{54}$$

Comparing Eqs. 53 and 54 shows that β_i is

$$\beta_i = \frac{p-1}{\left(p - \dfrac{1}{\bar{v}_1} \displaystyle\sum_{j=1}^{i-1} \bar{v}_j b_{ji} \right)}. \tag{55}$$

Then, δ_i can be obtained by substituting Eq. 55 into 51:

$$\delta_i = \frac{(p-1) \dfrac{1}{\bar{v}_i} \displaystyle\sum_{j=1}^{i-1} \bar{v}_j b_{ji}}{p - \dfrac{1}{\bar{v}_i} \displaystyle\sum_{j=1}^{i-1} \bar{v}_j b_{ji}}. \tag{56}$$

In all cases, the discretized breakage distribution function is $b_{ij} = B(v_i, v_{j-1}) - B(v_{i-1}, v_{j-1})$ and the cumulative breakage function $B(v, w)$ is

$$B(v,w) = \int_0^v b'(u,w)\, du. \tag{57}$$

Applying these definitions to the product function Eq. 39 yields the following expression:

$$b_{ij} = \frac{p(z+m+1)!}{m!z!} \sum_{k=0}^{z} \binom{z}{k} (-1)^k \frac{1}{k+m+1} \left[\left(\frac{v_i}{v_{j-1}} \right)^{k+m+1} - \left(\frac{v_{i-1}}{v_{j-1}} \right)^{k+m+1} \right], \tag{58}$$

where $z = m + (m+1)(p-2)$. Similarly, for the summation function Eq. 46, we get

$$b_{i,j} = A_{m,p} \left\{ \prod_{n=0}^{p-3} \frac{1}{n+1} \sum_{k=0}^{p-2} \binom{p-2}{k} (-1)^k \frac{1}{k+m+1} \times \left[\left(\frac{v_i}{v_{j-1}} \right)^{k+m+1} - \left(\frac{v_{i-1}}{v_{j-1}} \right)^{k+m+1} \right] + \left(\frac{p-1}{A_{m,p-1}} \right) \sum_{k=0}^{m+p-2} \times \binom{m+p-2}{k} (-1)^k \frac{1}{k+1} \left[\left(\frac{v_i}{v_{j-1}} \right)^{k+1} - \left(\frac{v_{i-1}}{v_{j-1}} \right)^{k+1} \right] \right\}. \tag{59}$$

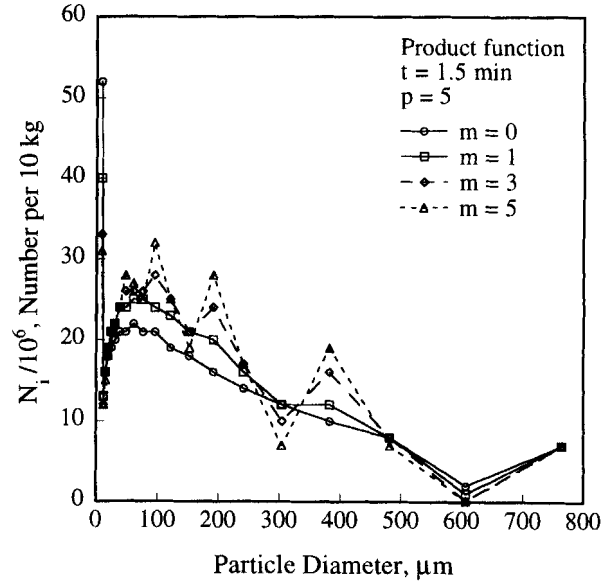

(a)

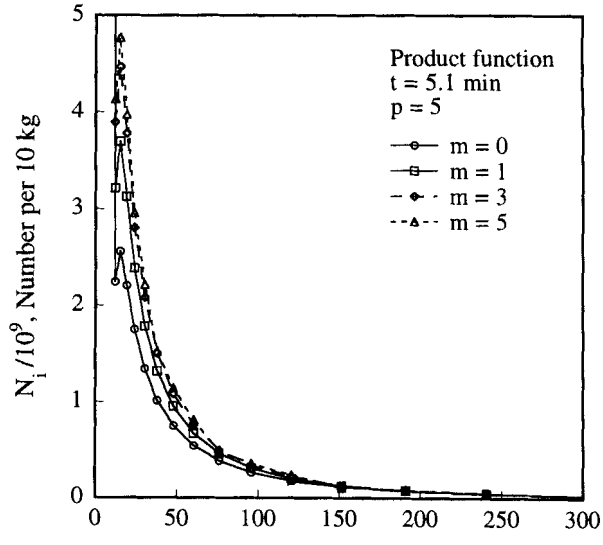

(b)

Figure 7. PSD for the product function with $p = 5$ and various values of m: (a) at 1.5 min; (b) at 5.1 min.

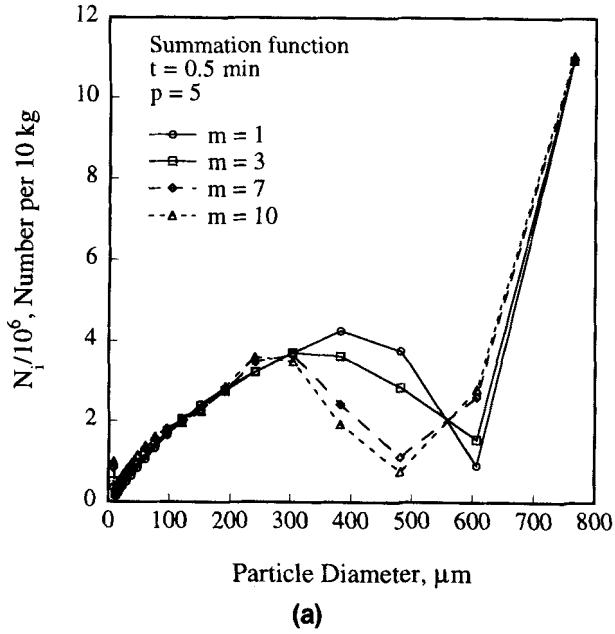

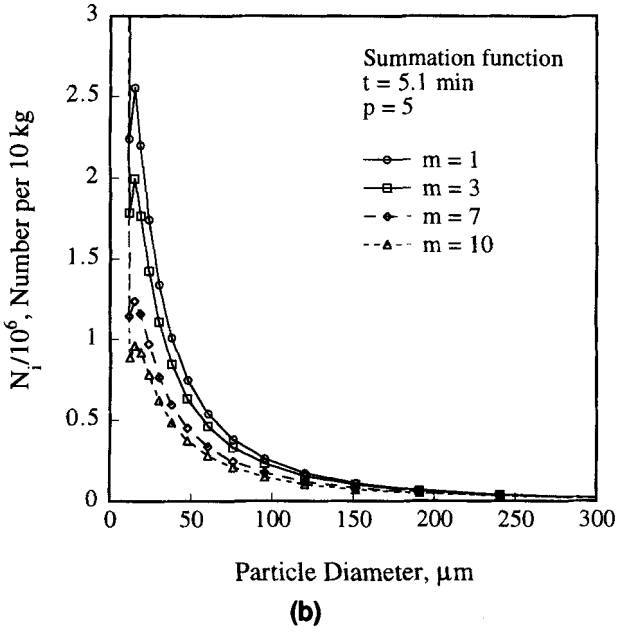

Figure 8. PSD for the summation function with $p = 5$ and various values of m: (a) at 0.5 min; (b) at 5.1 min.

Equations 50, 55, 56, 58 and 59 are applicable for both equal- and geometric-size intervals. They ensure the correct prediction of the total number of particles and conservation of mass.

Results

Simulations are performed with both the product and summation functions to show the effect on the resulting PSD. In these simulations, 20 geometric size intervals with a geometric ratio of 2 are used and the maximum particle size in interval 1, v_1, is 10.4 μm. An initial charge of 10 kg of particles is evenly distributed with respect to volume and is in the top size range between 667 and 841 μm in diameter. The specific

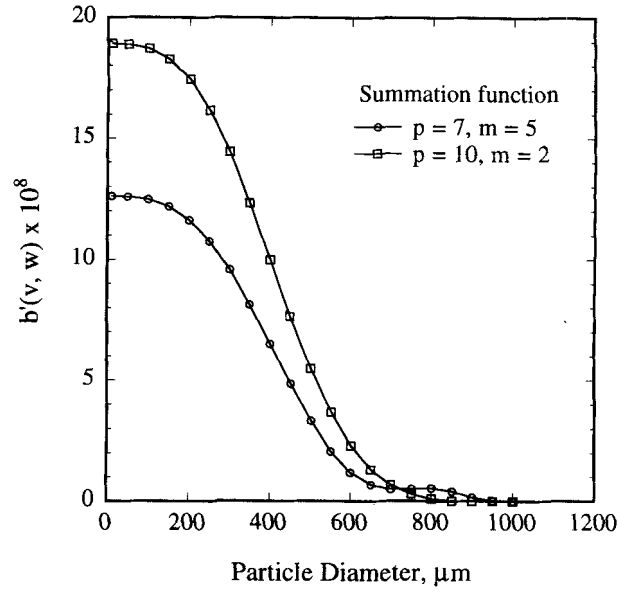

Figure 9. Summation breakage distribution function for: $p = 7$ with $m = 5$; $p = 10$ with $m = 2$.

rate of breakage is zero for the first interval and is a constant of 0.56 min^{-1} for all other size intervals. The particle density is 3.217 g/cm^3, the density of silicon carbide.

In the first set of simulations, the effect of the exponent, m, of the product function for $p = 5$ is investigated. Figure 7a shows that the PSDs for various values of m at 1.5 minutes are easily distinguishable. The jagged peaks can be explained as follows. With the initial size distribution being a rectangular pulse in the top size interval, the initial breakage causes a second peak to form as indicated by $b'(v, w)$. Then, as breakage progresses, the particles in the second peak start breaking and form a third peak. As grinding continues, several peaks are formed. As m is increased, the peaks become higher and sharper (Figure 2). After sufficient grinding, it is expected that these peaks would overlap to the point that a smooth curve is produced. Indeed, Figure 7b shows that at 5.1 minutes the PSD changes little with m. The effect of the power-law exponent of the summation function on PSD is shown for 0.5 and 5.1 minutes of grinding in Figures 8a and 8b, respectively. Again, the effect on PSD is more pronounced at short times.

Previously, we showed that the empirical distribution function is probably made up of a number of theoretical functions. To match the data, however, we had to assume that occasionally up to 5,000 child particles are formed per breakage. If one believes that 5,000 particles are too many to be physically realistic, we offer the following alternate explanation. Consider two easily distinguishable summation form breakage distribution functions, one for $p = 7$ and $m = 5$ and the other for $p = 10$ and $m = 2$ (Figure 9). Let us further assume that the former has a breakage rate of 0.82 min^{-1} and the latter 0.56 min^{-1}. Recall that breakage data are often reported as a plot of the cumulative mass distribution as a function of particle diameter at various times. Figure 10 shows that the two distributions with different parameters produce almost identical cumulative mass distributions. Therefore, it is probable that the empirical distribution functions could

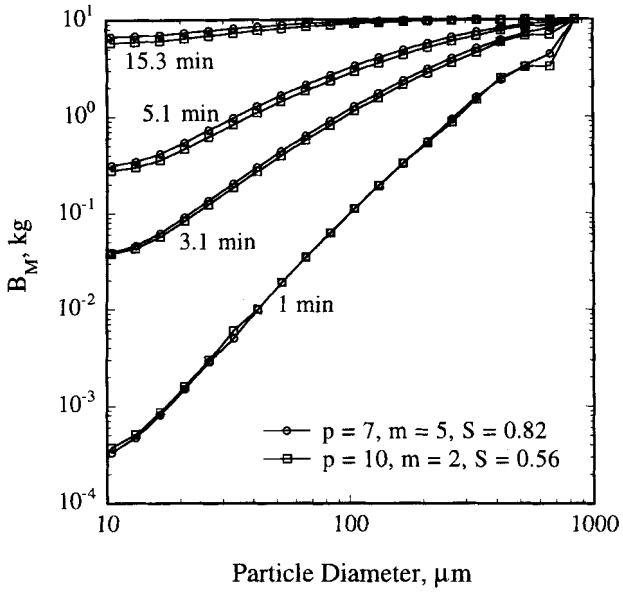

Figure 10. PSD after 1.5, 3.1, 5.1 and 15.3 min of grinding for two cases of the summation function where $p=7$ with $m=5$ and $p=10$ with $m=2$.

have been lowered at the small particle end while raising the specific rate of breakage in the back calculations.

Conclusions

Breakage is a complex and diverse phenomenon. In chemical engineering practice, it may be an important factor in the design of plants with solids processing steps (Rajagopal et al., 1992; Ennis et al., 1995). However, a complete mechanistic understanding of solids breakage is not yet available despite all the fundamental studies (Yashima et al., 1987; Ghadiri et al., 1991). The problem is further compounded by the fact that breakage may be history-dependent, with the solid fracturing along existing cracks. It is clear that for the foreseeable future the use of empirical specific rate of breakage and distribution function is essential in quantifying breakage in process equipment.

To meet this need, we have worked out a procedure for developing theoretical breakage functions that produce exactly p child particles with each breakage. This method is demonstrated with both a product and a summation power-law form function, although other functional forms can be used. It is shown that not only can the theoretical functions represent experimental data, but they also offer the advantages below.

Based on a comparison of the theoretical and empirical functions, we conclude that, as expected, each breakage may result in a very different number of child particles. Furthermore, an empirical breakage function may be physically unrealistic in that there is no minimum particle size below which breakage is no longer possible (Kendall, 1978) and in that an infinite number of child particles are produced each time a parent particle is broken. These problems are eliminated with the product form of the theoretical distribution function when m equals unity, which predicts no particles with zero volume. In addition, a companion discretized breakage equation for use with the theoretical distribution has been developed. After discretization, Eq.1 becomes a set of ordinary differential equations, Eq. 50, which can be easily integrated. Conservation of mass and correct prediction of the total number of particles are guaranteed with the discretized breakage equation.

This current method provides additional flexibility and insights in modeling breakage data. However, it does not confront the inverse problem, namely, the determination of functional form for $b(v_1, v_2, \ldots, v_{p-1}, w)$ from experimental data on the PSD. This is important because various breakage function parameters can produce two very similar cumulative mass distribution functions. The work by Ramkrishna and coworkers (Wright and Ramkrishna, 1992; Sathyagal et al., 1995) provides a good starting point for this research. Another possible extension is to use basic material properties (Kelley and Macmillan, 1986) to screen and evaluate candidate theoretical functions.

Finally, it should be mentioned that other approaches can be used to model breakage. By using three and six interlaced Fibonacci series (Chang et al., 1991; Zhang et al., 1991, 1992), ternary breakage for discrete particle sizes is modeled. Another promising method is the use of stochastic population balance (Chen et al., 1994), which is suitable for a system with a limited number of particles. Clearly, the statistics of multiple particle breakage awaits additional research.

Acknowledgment

The support of the National Science Foundation (Grant CTS-9211673) for this research is gratefully acknowledged.

Notation

g = arbitrary function
h, i, j, k, n, z = positive integers
m_j = jth moment
$P(v)$ = number of child particles formed between size v and the parent particle size
S_c = constant for the rate of breakage, $\mu m^{-3\alpha}$ min^{-1}
S_i = discretized volume-based specific rate of breakage, min^{-1}
u = particle volume, μm^3

Greek letters

α = exponential factor in specific rate of breakage
β' = constant in empirical breakage function
γ = constant in empirical breakage function
η = constant in suggested breakage function
λ = constant in suggested breakage function
ϕ = constant in empirical breakage function

Subscripts

i, j = size intervals
M = mass basis

Literature Cited

Austin, L. G., and P. T. Luckie, "Methods for Determination of Breakage Distribution Parameters," *Powder Tech.*, **5**, 215 (1971/72a).

Austin, L. G., and P. T. Luckie, "The Estimation of Non-Normalized Breakage Distribution Parameters from Batch Grinding Tests," *Powder Tech.*, **5**, 267 (1971/72b).

Austin, L., K. Shoji, V. Bhatia, V. Jindal, K. Savage, and R. Klimpel, "Some Results on the Description of Size Reduction as a Rate Process in Various Mills," *Ind. Eng. Chem. Proc. Des. Dev.*, **15**, 187 (1976).

Chang, Y-C., R. V. Calabrese, and J. W. Gentry, "An Algorithm for

Determination of the Size-Dependent Breakage Frequence of Droplets, Flocs and Aggregates," *Part. Part. Syst. Charact.*, **8,** 315 (1991).
Chen, W.-Y., G. Nagarajan, Z. P. Zhang, B. C. Shen, and L. T. Fan, "Stochastic Modeling of Devolatilization-Induced Coal Fragmentation during Fluidized-Bed Combustion," *Ind. Eng. Chem. Res.*, **33,** 137 (1994).
Davis, H. T., "On the Statistics of Randomly Broken Objects," *Chem. Eng. Sci.*, **44,** 1799 (1989).
Ennis, B. J., J. Green, and R. Davies, "Particle Technology: The Legacy of Neglect in the U.S.," *Chem. Eng. Prog.*, **90,** 32 (1995).
Feller, W., *An Introduction to Probability Theory and Its Applications*, Wiley, New York (1966).
Ghadiri, M., K. R. Yuregir, H. M. Pollock, J. D. J. Ross, and N. Rolfe, "Influence of Processing Conditions on Attrition of NaCl Crystals," *Powder Tech.*, **65,** 311 (1991).
Glasgow, L. A., and R. H. Luecke, "Mechanisms of Deaggregation for Clay-Polymer Flocs in Turbulent Systems," *Ind. Eng. Chem. Fundam.*, **19,** 148 (1980).
Grady, D. E., "Particle Size Statistics in Dynamic Fragmentation," *J. Appl. Phys.*, **68,** 6099 (1990).
Hill, P. J., and K. M. Ng, "New Discretization Procedure for the Breakage Equation," *AIChE J.*, **41,** 1204 (1995).
Hoare, M., T. J. Narendranathan, J. R. Flint, D. Heywood-Waddington, D. J. Bell, and P. Dunnill, "Disruption of Protein Precipitates during Shear in Couette Flow and in Pumps," *Ind. Eng. Chem. Fundam.*, **21,** 402 (1982).
Jolley, L. B. W., *Summation of Series*, Dover, New York (1961).
Karabelas, A. J., "Particle Attrition in Shear Flow of Concentrated Slurries," *AIChE J.*, **22,** 765 (1976).
Kelley, A., and N. H. Macmillan, *Strong Solids*, 3rd Ed., Clarendon Press, Oxford (1986).
Kendall, K., "The Impossibility of Comminuting Small Particles by Compression," *Nature*, **272,** 710 (1978).
Klimpel, R. R., and L. G. Austin, "Determination of Selection-for-Breakage Functions in the Batch Grinding Equation by Nonlinear Optimization," *Ind. Eng. Chem. Fundam.*, **9,** 230 (1970).
Klimpel, R. R., and L. G. Austin, "The Back-Calculation of Specific Rates of Breakage from Continuous Mill Data," *Powder Tech.*, **38,** 77 (1984).
Kusters, K. A., S. E. Pratsinis, S. G. Thoma, and D. M. Smith, "Ultrasonic Fragmentation of Agglomerate Powders," *Chem. Eng. Sci.*, **48,** 4119 (1993).
Masiuk, S., "Power Consumption, Mixing Time and Attrition Action for Solid Mixing in a Ribbon Mixer," *Powder Tech.*, **51,** 217 (1987).
Mazzarotta, B., "Abrasion and Breakage Phenomena in Agitated Crystal Suspensions," *Chem. Eng. Sci.*, **47,** 3105 (1992).
Nienow, A. W., and R. Conti, "Particle Abrasion at High Solids Concentration in Stirred Vessels," *Chem. Eng. Sci.*, **33,** 1077 (1978).
Offermann, H., and J. Ulrich, "On the Mechanical Attrition of Crystals," *Industrial Crystallization 81*, S. J. Jancic and E. J. de Jong, eds., North-Holland, New York (1982).
Rajagopal, S., K. M. Ng, and J. M. Douglas, "A Hierarchical Procedure for the Conceptual Design of Solids Processes," *Comput. Chem. Eng.*, **16,** 675 (1992).
Sathyagal, A. N., D. Ramkrishna, and G. Narsimhan, "Solutions of Inverse Problems in Population Balances—II. Particle Break-Up," *Comput. Chem. Eng.*, **19,** 437 (1995).
Shook, C. A., D. B. Haas, W. J. W. Husband, and M. Small, "Breakage Rates of Lignite Particles During Hydraulic Transport," *Can. J. Chem. Eng.*, **56,** 448 (1978).
Synowiec, P., A. G. Jones, and P. A. Shamlou, "Crystal Break-up in Dilute Turbulently Agitated Suspensions," *Chem. Eng. Sci.*, **48,** 3485 (1993).
Wei, J., W. Lee, and F. J. Krambeck, "Catalyst Attrition and Deactivation in Fluid Catalytic Cracking System," *Chem. Eng. Sci.*, **32,** 1211 (1977).
Wright, H., and D. Ramkrishna, "Solutions of Inverse Problems in Population Balances—I. Aggregation Kinetics," *Comput. Chem. Eng.*, **16,** 1019 (1992).
Yashima, S. Y., Y. Kanda, and S. Sano, "Relationships between Particle Size and Fracture Energy or Impact Velocity Required to Fracture as Estimated from Single Particle Crushing," *Powder Tech.*, **51,** 277 (1987).
Zhang, N., R. V. Calabrese, and J. W. Gentry, "Fundamental Properties of Interlaced Fibonacci Sequences and their Potential in Describing Particle Breakage," *J. Aerosol. Sci.*, **23,** S193 (1992).
Zhang, N., Y.-C. Chang, R. V. Calabrese, and J. W. Gentry, "The Use of Fibonacci Sequences to Model Ternary Breakages," *J. Aerosol. Sci.*, **22,** S223 (1991).
Ziff, R. M., "New Solutions to the Fragmentation Equation," *J. Phys. A: Math. Gen.*, **24,** 2821 (1991).

Manuscript received July 5, 1995, and revision received Oct. 20, 1995.